Available online at www.sciencedirect.com
ScienceDirect
Ceramics International 37 (2011) 3365–3370
CERAMICS INTERNATIONAL
www.elsevier.com/locate/ceramint

Morphology control and growth mechanism of magnesium hydroxide nanoparticles via a simple wet precipitation method

Peipei Wang, Caihong Li *, Haiyan Gong, Hongqiang Wang, Jinrong Liu

School of Chemical Engineering, Inner Mongolia University of Technology, Hohhot 010051, PR China

Received 29 April 2011; accepted 25 May 2011
Available online 1 June 2011

Abstract

The nanograde particles of magnesium hydroxide [$Mg(OH)_2$] with needle-like and disk-like morphologies were synthesized via a simple wet precipitation method. The effects of operation parameters, such as ammonia concentration, Mg^{2+} concentration, reaction temperature and ageing temperature on morphology of magnesium hydroxide nanoparticles were investigated. The samples were characterized by transmission electron microscopy (TEM), Fourier transform infrared spectroscopy (FTIR) and X-ray diffractions (XRD). The influence process and growth mechanism were discussed in details.

Keywords: Crystal morphology; Growth from solution; Nanomaterials; Magnesium hydroxide

1. Introduction

Magnesium hydroxide [$Mg(OH)_2$] has been attracted much attention, for its widely application in flame-retardant fields and environment protection [1–4]. As a new flame-retardant filler, $Mg(OH)_2$ are widely used in polymeric materials, and it has been found that the addition of $Mg(OH)_2$ additives caused a dramatic decrease in impact toughness [5]. While nanoneedles and nanolamellas can be good candidates for functional polymeric composites and fiber hybrid materials which are usually used as reinforcing agents or halogen-free retardants [6]. Generally, the shape, particle size, particle size distribution and dispersibility were strongly dependent on the preparation process of $Mg(OH)_2$ [7–9]. So far, $Mg(OH)_2$ crystals with various morphologies, such as plates, lamellar, rod, needle-like and so on, were synthesized by means of bubbling setup [10], wet coprecipitation [11], and hydrothermal method [12]. For all the preparing method, wet precipitation was proved to be the most simple and low-cost way to synthesize $Mg(OH)_2$ crystals.

In this paper, nanograde $Mg(OH)_2$ crystals with special morphologies were synthesized via a simple wet method. The synthesis parameters influencing on the morphology, particle size of $Mg(OH)_2$ were investigated, such as reactant concentration, reaction and ageing temperature. The influence process and the growth mechanism of $Mg(OH)_2$ were discussed in details.

2. Experimental

2.1. Materials

All chemicals used in this work, such as magnesium chloride ($MgCl_2{\cdot}6H_2O$), aqueous ammonia ($NH_3{\cdot}H_2O$), polyethyleneglycol-12000 (PEG-12000) were of A.R. grade and were used directly without further purification.

2.2. Synthesis method of $Mg(OH)_2$ nanoparticles

$Mg(OH)_2$ nanoparticles were synthesized by a simple wet precipitation method under atmospheric pressure with PEG-12000 added as a dispersant. The parameters of the experiments are summarized in Table 1. The molar ratio $n(OH^-)/n(Mg^{2+})$ was maintained at 2.2 in all of the cases. In a typical procedure (for sample a), $MgCl_2{\cdot}6H_2O$ was solved in distilled water and the concentration of $MgCl_2$ was 1.5 mol L^{-1}. 50 ml $MgCl_2$ solution was added into a 250 ml three-necked flask, with 0.1 g PEG-12000 added as dispersant, and then the flask was placed

* Corresponding author at: No.49, Aimin Street, Xincheng Area, Hohhot, Inner Mongolia 010051, China. Tel.: +86 471 6575722; fax: +86 471 6575722.
E-mail address: licaihong1967@yahoo.com.cn (C. Li).

0272-8842/$36.00
doi:10.1016/j.ceramint.2011.05.138

Table 1
Sample codes of $Mg(OH)_2$ and reaction conditions.

Sample code	Concentration of ammonia (wt.%)	Concentration of $MgCl_2$ (mol L^{-1})	Reaction temperature (°C)	Ageing temperature (°C)
A	5	1.5	40	20
B	15	1.5	40	20
C	25	1.5	40	20
D	15	0.5	40	20
E	15	2.5	40	20
F	15	0.5	20	20
G	15	0.5	60	20
H	15	0.5	80	20
I	15	0.5	40	40
J	15	0.5	40	60

into the ultrasound bath to promote solid state PEG dissolving in the solution of magnesium chloride. Then 5 wt.% $NH_3 \cdot H_2O$ was dropped into the mixture slowly. The mixture was stirred at a speed of 300 rpm, and the reaction temperature was maintained at 40 °C for about 1–1.5 h. The resulted suspension was naturally cooled to room temperature (20 °C), aged for 24 h, and then filtered. The solid product was washed with distilled water and then was washed with absolute ethanol several times. The product was dried at 80 °C for 5 h.

2.3. Measurements

The crystal phase and the degree of crystallinity were characterized by X-ray diffraction (XRD, D8-Advance, Bruker company, Germany), using Cu Kα radiation (λ = 0.15418 nm) at the X-ray tube voltage 40 kV and tube current 40 mA. The XRD data were collected at room temperature over the 2θ range of 20–55° at a step size of 0.02°/s and a count time of 0.06 s/step. The typical groups of $Mg(OH)_2$ were analyzed by Fourier transform infrared spectroscopy (FTIR). The morphology of the sample was studied by transmission electron microscope (TEM, JEM-2010, JEOL Ltd.).

3. Results and discussion

3.1. Effect of ammonia concentration

$Mg(OH)_2$ samples prepared with ammonia concentrations selected were analyzed by TEM, as shown in Fig. 1. Three samples a, b and c show morphology of nanograde needle, although with different sizes, with 200 nm × 15 nm (Fig. 1a), 800 nm × 50 nm (Fig. 1b) and 650 nm × 70 nm (Fig. 1c). There coexist some disks and nanorods in the sample c, which was prepared with 25 wt.% ammonia.

In this work, nanoneedles rather than irregularly shaped lamellae were obtained. This is attributed to the addition of PEG-12000 which prevented the agglomeration. When the nucleation rate is higher than the growth rate, the consumption of supersaturation is mainly on nucleation, and finally, large amount of fine crystals are obtained. Conversely, when the growth rate is higher, the consumption of supersaturation is mainly on particles growth rather than on nucleation, and large size crystal particles are obtained. The particle sizes had a slight change as the ammonia concentration changed, because of the relative magnitude of nucleation and crystal growth rate affected by ammonia concentration [13]. That was why the sample prepared with 25 wt.% showed smaller particle size than that prepared with 15 wt.% ammonia. Compared to the sample prepared with 15 wt.% ammonia, the samples prepared with 5 wt.% also showed a smaller size. That was because both nucleation and crystal growth rate were lower caused by the lower supersaturation, which caused smaller crystal size.

It should be mentioned that there coexist three morphologies, needle-, disk- and rod-like, in the sample c which was prepared with 25 wt.% ammonia. This was attributed to the high concentration ammonia and bad micromixing, which caused heterogeneous supersaturation of solution. Thus, the relative growth rates of individual faces of $Mg(OH)_2$ crystals were strongly affected and then the final morphologies changed.

3.2. Effect of Mg^{2+} concentration

It was found that the Mg^{2+} concentration investigated mainly influenced the dispersibility of the nanoneedles of $Mg(OH)_2$. With the increase of Mg^{2+} concentration, the nanocrystals agglomeration became more serious. What was more interesting, the crystal particles showed a broom shape (Fig. 2e), as the Mg^{2+} concentration was 2.5 mol L^{-1}. It might be determined by the relation of surface diffusion and surface integration in the crystal growth process. When a crystal is growing from supersaturation solution, solute is leaving the solution at the solid–liquid interface and becoming the part of the crystal. Crystal growth proceeds on a molecular level by the sequential addition of growth units (single solute molecules, ions, or atoms, or possibly clusters of these) to the crystal lattice. Close to the interface, transport is restricted by molecular diffusion through a diffusion boundary layer, irrespective of the convective conditions outside this region. After the solute molecules diffuse from the bulk liquid phase to the interfacial region, they are adsorbed on the surface of solid, and under some circumstances, diffuse two-dimensionally on the surface before being integrated into the crystal lattice. During the surface diffusion step, bonds between the solute and solvent molecules are broken, which free the solute to form bonds with the surface molecules of the crystal, and thus the process for solute molecule integrating into the crystal lattice complete. As the diffusion rate was higher than that of the surface integration, the growth units could not get enough time

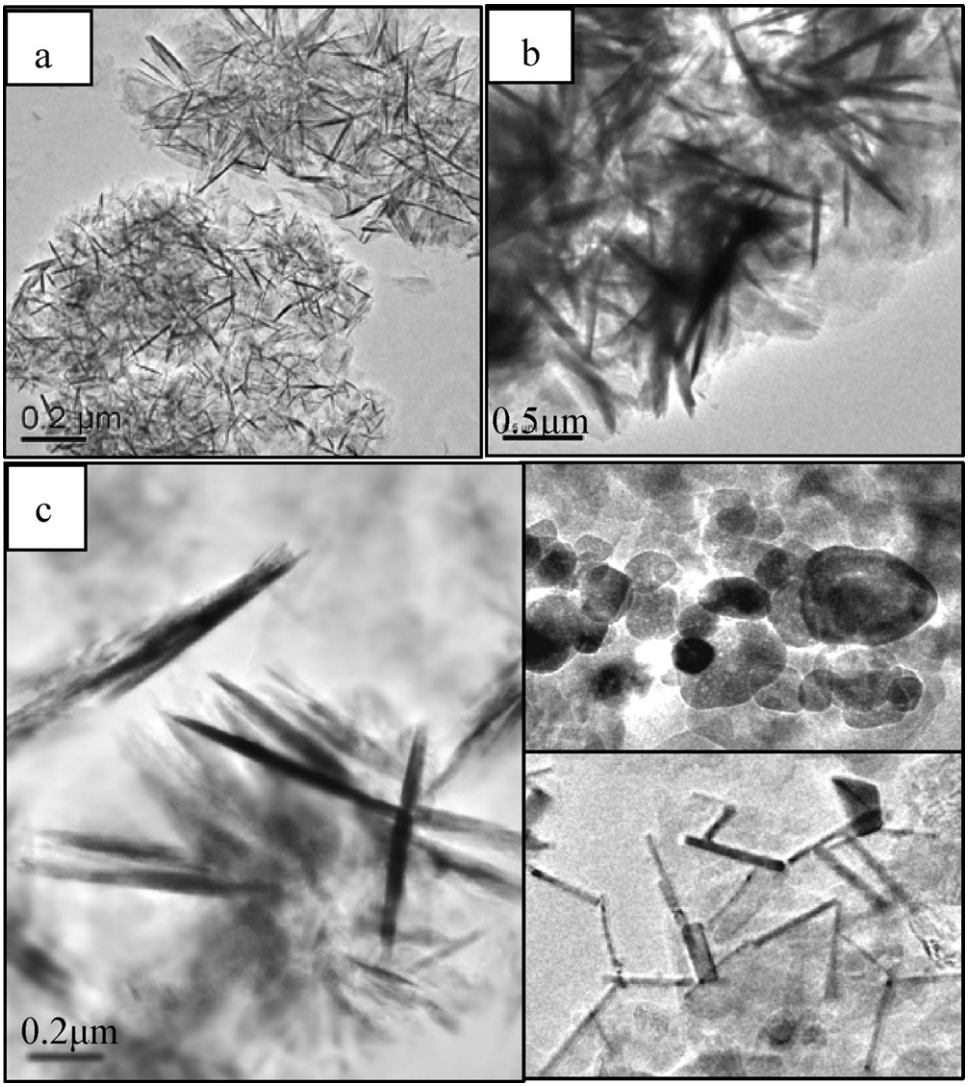

Fig. 1. TEM images of samples prepared with different concentration of ammonia: (a) 5 wt.%, (b) 15 wt.%, and (c) 25 wt.%.

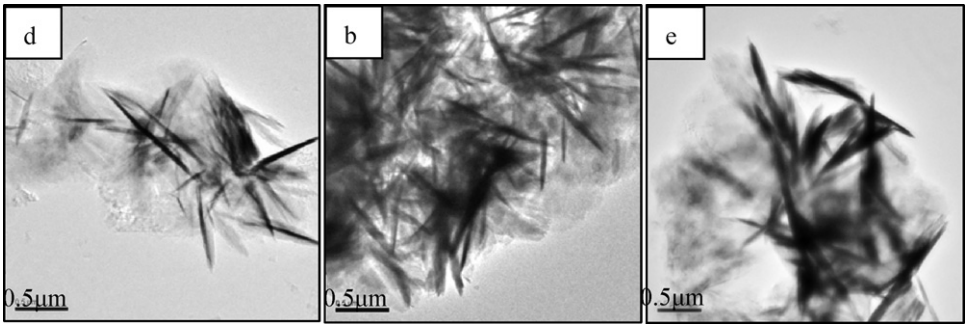

Fig. 2. TEM images of samples prepared with different concentration of Mg^{2+}: (d) 0.5 mol L^{-1}, (b) 1.5 mol L^{-1}, and (e) 2.5 mol L^{-1}.

to add to the crystal lattice, exactly following the ordering rule. And thus, the crystal formed a broom rather than a needle with regular transect.

3.3. Effect of reaction temperature

The reaction temperature plays an important role on controlling the morphology and particle size of $Mg(OH)_2$ crystal, as shown in Fig. 3. Nanoneedles were prepared at 20 °C (340 nm × 20 nm) and 40 °C (800 nm × 50 nm), while nanodisks (with a diameter about 50–200 nm) with a few nanoneedles at 60 °C and nanodisks (with a diameter about 200 nm) absolutely at 80 °C.

Crystal growth refers to the process that the nuclei grow larger by the addition of solute molecules from the supersaturated solution to the crystal lattice. The shape of a crystal is

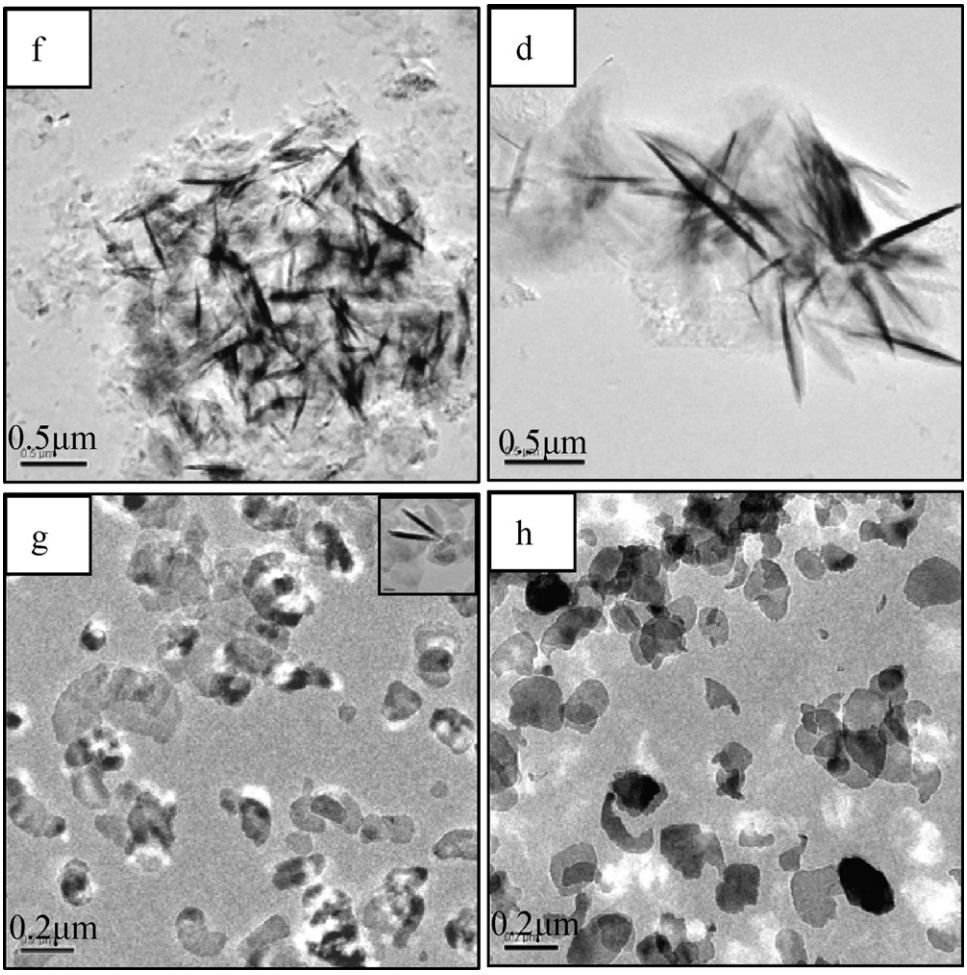

Fig. 3. TEM images of samples prepared at different reaction temperatures: (f) 20 °C, (d) 40 °C, (g) 60 °C, and (h) 80 °C.

determined by the relative growth rates of individual faces of the crystal, which can be strongly influenced by the presence of impurities, and even the solvent itself. During crystallization, fast growing faces normally grow out of existence, leaving the crystal bounded by the slowest growing faces. Impurities or solvents that adsorb or interact with the crystal face in such a way to slow the grow rate can further increase its relative area [14]. To a large degree, the process of impurity adsorption, diffusion, and integration is analogous to the growth process by solute transport and integration at the interface. Accordingly, the relative ''mobility'' of impurity on the crystal surface, and its tendency to incorporate in the crystal lattice, depend on a number of factors that are influenced by temperature and(or) supersaturation [14]. In this work, PEG-12000 played a role of dispersant and template, and temperature was the most important factor that might influence the adsorption modes of PEG-12000 on the crystal faces of $Mg(OH)_2$ (as shown in Fig. 4). When the temperature was at 40 °C and 20 °C, PEG-12000 was adsorbed on the crystal faces that paralleled with the *c* axis, which prevented the solute diffusion to the faces, so the crystal grew along one dimension to form nanoneedles of $Mg(OH)_2$ as shown in mode A in Fig. 4. When the temperature was 60 °C and 80 °C, PEG-12000 was adsorbed on the crystal faces (0 0 1), and then the crystal was limited to grow along the face of (0 0 1), and thus, nanodisks of $Mg(OH)_2$ were obtained as shown in mode B in Fig. 4.

The FTIR was recorded to study the interaction between magnesium hydroxide and PEG-12000. As shown in Fig. 5, the sharp and intense peak at 3696 cm^{-1} was due to the OH group in $Mg(OH)_2$. The bands in the range of 1400–1630 cm^{-1} were attributed to the –OH stretching mode in water. The broad band at 3431 cm^{-1} was attributed to surface

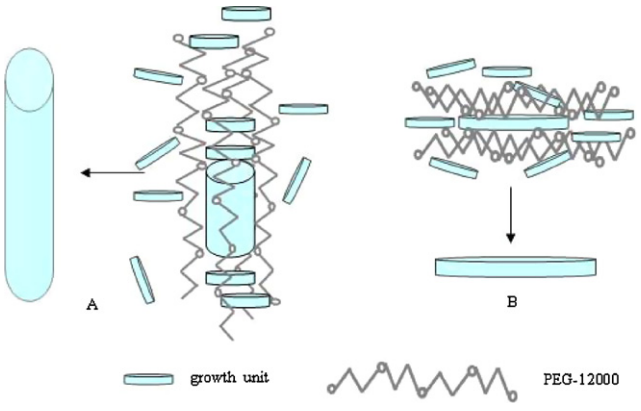

Fig. 4. Schematic diagram of the adsorption modes of PEG-12000 influenced by temperature: (A) 40 °C and 20 °C and (B) 60 °C and 80 °C.

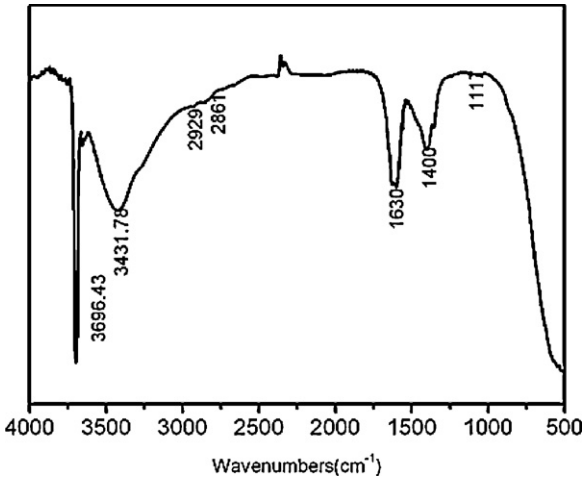

Fig. 5. FTIR patterns of sample e.

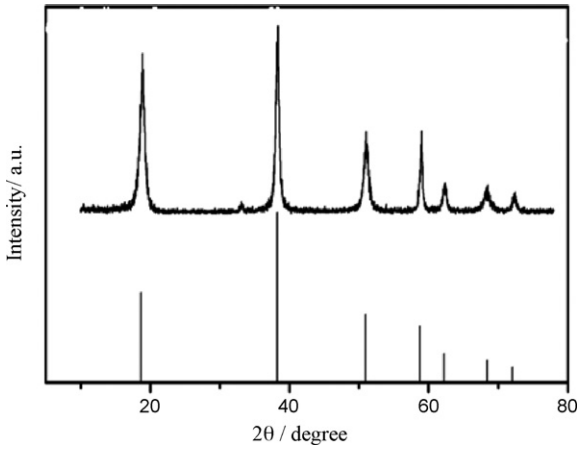

Fig. 6. XRD patterns of sample e.

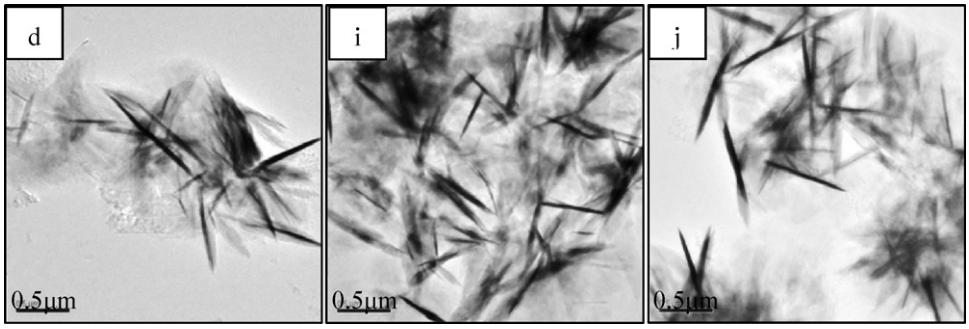

Fig. 7. TEM images of samples prepared at different ageing temperatures: (d) 20 °C, (i) 40 °C, and (j) 60 °C.

adsorbed –OH groups of PEG-12000, and the weak peaks at 2929 cm^{-1} and 2861 cm^{-1} were due to the $–CH_2$ of PEG-12000, and the band at 1117 cm^{-1} was attributed to the C–O–C asymmetric stretching vibration of PEG-12000. The results of FTIR showed that PEG-12000 was adsorbed on the surface of $Mg(OH)_2$ crystal.

The sample was further analyzed by XRD, as shown in Fig. 6. All the diffraction peaks can be indexed as hexagonal phase $Mg(OH)_2$ according to the standard data JCPDS 01-1169. In addition, no characteristic peaks of other impurities were observed, which indicated that the product had a high purity.

3.4. Effect of ageing temperature

The samples prepared at different ageing temperature were analyzed by TEM, as shown in Fig. 7. The pictures indicated that ageing temperature had little effect on the morphology of $Mg(OH)_2$ crystal, but influenced the crystals' dispersibility. With the ageing temperature increasing. $Mg(OH)_2$ nanoneedles showed a better dispersibility, and the particle size became larger. This was because the fine crystals dissolved and the large crystals grew during the ageing process. Higher ageing temperature might be beneficial to accelerate the rate of the process of diffusion and integration, and thus, the particle size became a bit larger.

4. Conclusions

Magnesium hydroxide nanoparticles with needle, disk-like morphologies were synthesized via a simple wet method, by controlling the process conditions and using PEG-12000 as dispersant and template. The influence of synthesis parameters on the morphology of crystals were investigated, such as ammonia concentration, Mg^{2+} concentration, reaction temperature and ageing temperature. It has been shown that, when ammonia concentration was 25 wt.%, it was hard to obtain $Mg(OH)_2$ particles with uniform morphology. When Mg^{2+} concentration was too high, the crystal particles showed broom shape. The reaction temperature, which influenced the adsorption modes of PEG-12000 on the crystal faces, was an important parameter to control the morphology and particle size of $Mg(OH)_2$.

Acknowledgements

We acknowledge the financial support from the National Natural Science Foundation of China (Grant no. 50862006) and

the Natural Science Foundation of Inner Mongolia (Grant no. 20080404MS0211).

References

[1] X.L. Chen, J. Yu, S.Y. Guo, Structure and properties of polypropylene composites filled with magnesium hydroxide, J. Appl. Polym. Sci. 102 (2006) 4943–4951.
[2] J.P. Lv, L.Z. Qiu, B.J. Qu, Controlled growth of three morphological structures of magnesium hydroxide nanoparticles by wet preciptation method, J. Cryst. Growth 267 (2004) 676–684.
[3] S.Q. Chang, T.X. Xie, G.S. Yang, Morphology and mechanical properties of high-impact polystyrene/elastomer/magnesium hydroxide composites, J. Appl. Polym. Sci. 102 (2006) 5184–5190.
[4] T. Kameda, H. Takeuchi, T. Yoshioka, Preparation of organic acid anion-modified magnesium hydroxides by coprecipitation: a novel material for the uptake of heavy metal ions from aqueous solutions, J. Phys. Chem. Solids 70 (2009) 1104–1108.
[5] C.M. Tai, U. Robert, K.Y. Li, Studies on the impact fracture behaviour of flame retardant polymeric material, Mater. Des. 22 (2001) 15–19.
[6] D. An, X. Ding, Z. Wang, Y. Liu, Synthesis of ordered arrays of magnesium hydroxide nanoparticles via a simple method, Colloids Surf., A 356 (2010) 28–31.
[7] R. Giorgi, C. Bozzi, L.G. Dei, Nanoparticles of $Mg(OH)_2$: synthesis and application to paper conservation, Langmuir 21 (2005) 8495–8501.
[8] H. Xu, X.R. Deng, Preparation and properties of superfine $Mg(OH)_2$ flame retardant, Trans. Nonferrous Compos. Met. Soc. China 16 (2006) 488–492.
[9] Y. Clifford, T.T. Chia, H.C. Ming, Synthesis of magnesium hydroxide and oxide nanoparticles using a spinning disk reactor, Ind. Eng. Chem. Res. 46 (2007) 5536–5541.
[10] X. Li, C. Ma, J. Zhao, Z. Li, S. Xu, Y. Liu, Preparation of magnesium hydroxide nanoplates using a bubbling setup, Powder. Technol. 198 (2010) 292–297.
[11] D. Chen, L. Zhu, H. Zhang, K. Xu, M. Chen, magnesium hydroxide nanoparticles with controlled morphologies via wet coprecipitation, Mater. Chem. Phys. 109 (2008) 224–229.
[12] X.T. Sun, L. Xiang, Hydrothermal conversion of magnesium oxysulfate whiskers to magnesium hydroxide nanobelts, Mater. Chem. Phys. 109 (2008) 381–385.
[13] A.S. Myerson, R. Ginde, Crystals, crystal growth, and nucleation, in: A.S. Myerson (Ed.), Handbook of Industrial Crystallization, 2nd ed., Butterworth-Heinemanm, 2002, pp. 33–66.
[14] P.A. Meenan, S.R. Anderson, D.L. Klug, The influence of impurities and solvents on crystallization, in: A.S. Myerson (Ed.), Handbook of Industrial Crystallization, 2nd ed., Butterworth-Heinemann, 2002, pp. 67–100.